

CHARACTERIZATION OF DYNAMIC STALL PHENOMENON USING
TWO-DIMENSIONAL UNSTEADY NAVIER-STOKES EQUATIONS[†]

by

K.N. GHIA, U. GHIA* AND G.A. OSSWALD

Department of Aerospace Engineering and Engineering Mechanics

*Department of Mechanical, Industrial and Nuclear Engineering
University of Cincinnati, Cincinnati, Ohio 45221Contributions of this Study

Among the new significant aspects of the present work are (i) the treatment of the far-field boundary, (ii) the use of C-grid topology, with the branch-cut singularity treated analytically, (iii) evaluation of the effect of the envelope of prevailing initial states and, finally, (iv) the ability to employ streakline/pathline 'visualization' to probe the unsteady features prevailing in vortex-dominated flows. The far-field boundary is placed at infinity, using appropriate grid stretching. This contributes to the accuracy of the solutions, but raised a number of important issues which needed to be resolved; this includes determining the equivalent time-dependent circulation for the pitching airfoil. A secondary counter-clockwise vortex erupts from within the boundary layer and immediately pinches off the energetic leading-edge shear layer which then, through hydrodynamic instability, rolls up into the dynamic stall vortex. The streakline/pathline visualization serves to provide information for insight into the physics of the unsteady separated flow.

† This research is supported, in part, by AFOSR Grants (Nos. 87-0074 and 90-0249), with supercomputer resources being provided by the Ohio Supercomputer Center.

Physical Characteristics and Background

Specifically, the large amplitude rapid pitching motion associated with the initiation of a high angle-of-attack maneuver typically leads to the generation of a dynamic stall vortex whose evolution results in large transient lift, drag and moment that can, for short periods of time, produce loadings significantly larger than those expected during either steady, or quasi-steady flight. Indeed, the successful completion of an abrupt, drastic maneuver can depend upon the ability of holding the dynamic stall vortices in place, at least for the duration of the maneuver, and subsequently bleeding the excess accumulated vorticity in a controlled manner into the wake. Abrupt shedding of large amounts of locally concentrated vorticity can so rapidly alter the lift distribution on a body that a tumbling loss-of-control incident can occur, as the associated rapid changes in moment distribution cannot be tolerated.

Recently, Carr (1988) has comprehensively reviewed the literature on the dynamic stall phenomenon and has also articulated the effect of key parameters on this phenomenon. Helin (1989) has also highlighted recent advances in the field, while stressing the importance of unsteady aerodynamics for highly maneuverable and agile aircraft. In addition, he has raised the important issue of the effect of flow separation on the formation of the energetic dynamic-stall vortex. These two reviews adequately point out some of the unresolved issues associated with the problem of dynamic stall.

On the Analysis of Dynamic Stall

The unsteady Navier-Stokes analysis of K. Ghia, Osswald and Ghia (1985) and Osswald, K. Ghia and U. Ghia (1986) is modified to permit arbitrary three degree-of-freedom maneuvers, using body-fixed coordinates and a C-grid

topology. This formulation not only permits pitching motions, but also plunging and in-plane accelerating or decelerating motions; typically, the airfoil is pitched about the quarter-chord axis. The problem is formulated using vorticity and stream function as dependent variables in a non-using body-fixed reference frame in generalized coordinates. This formulation offers the important advantage over the primitive-variable formulation that the form of the governing equations in inertial and non-inertial reference frames is identical. The far-field boundaries are located at true infinity for this subsonic flow with its fully elliptic nature. The conformal mapping techniques used lead to analytical determination of the corresponding inviscid flow; this inviscid flow constitutes the true far-field boundary condition; by contrast, the studies of Visbal and Shang (1988) and Ekaterinaris (1989) place the far-field boundary at a finite distance from the airfoil, and employ free-stream conditions on the upstream boundary and zero streamwise gradients downstream. The present study uses an analytically determined clustered conformal grid, thereby avoiding numerical error in the computation of the metrics. The C-grid topology employed introduces a singularity at the trailing edge (TE) and all along the branch cut. For the latter, this singularity is treated using the method of analytic continuation, as developed by Osswald, K. Ghia and U. Ghia (1985). The conditions of zero slip and zero normal velocity at the surface of the airfoil are implemented appropriately in terms of the stream function and vorticity. At the TE, the singularity in the grid does play a role in determination of the stream function, which is obtained by satisfying the Kutta condition. The vorticity at the TE is determined using the analysis of Osswald, K. Ghia and U. Ghia (1989). The direct numerical simulation (DNS) methodology developed by the authors is used to solve the

vorticity transport and stream function equations. Central differences are used for all spatial derivatives and no artificial dissipation is added explicitly.

Results and Discussion

In the present study, simulations are carried out for a NACA 0015 airfoil undergoing constant $\dot{\theta}$ -pitch-up motion. Two flow configurations are attempted and they are for $Re = 10^3$ and 10^4 . Configuration I, with the lower $Re = 10^3$, is used in the development phase, since it permits the use of a smaller grid (274, 76) of which 114 grid points are placed on the body. On the other hand, configuration II, with $Re = 10^4$, is used to compare the results of the experiments of Walker, Helin and Strickland (1985) who considered $Re = 45000$. This latter configuration was run using a (444,101) grid with 204 grid points on the body; the size of the grid was selected based on the results of Visbal and Shang (1988) who had carried out a grid study and selected this size. In addition, the same constant $\dot{\theta}$ -pitch-up motion as used by them is also implemented here and corresponds to nondimensional pitch rate $\Omega_0 = 0.2$ with nondimensional acceleration time $t_0 = 0.5$, and pivot axis location measured from airfoil leading edge $x_0 = 0.25$.

Results of configuration I, in Fig. 1, show that the dynamic stall vortex with its clockwise spinning fluid evolves as the shear layer from the leading edge is pushed away by the counterclockwise spinning vortex close to the body surface and subsequently the shear layer rolls up and forms a dynamic stall vortex. It appears that the eruption of counterclockwise spinning vortex from within the boundary layer is important to formation of the dynamic stall vortex near the leading edge.

Results for configuration II, in Fig. 2, show that $\theta = 0^\circ$ run exhibits unsteady results as opposed to the steady-state results obtained by Visbal and Shang. Their steady-state solutions could strictly be a consequence of the use of both explicit as well as implicit smoothing, i.e., artificial viscosity, to maintain stability in their numerical calculations, which employed the method of Beam and Warming. Present results for configuration II, although not depicted here, show that there are grid related oscillations near the leading edge in the vorticity contours and grid structure and perhaps its density needs to be altered before generating new results and analyzing them. Still, in this case, also the secondary counterclockwise vortex erupts from within the boundary layer on the surface to form the dynamic stall vortex. Unlike wind-tunnel tests, the numerical, experiment in the present study computes the vorticity field directly. By evaluating various individual terms in the vorticity- transport equation, it is possible to examine vorticity accumulation and generation at the body surface as well as in the flux from the boundary to reveal the underlying mechanism and the role of unsteady separation on the evolution of the stall vortex. This is possible once a comprehensive set of results are obtained.

In summarizing, the constant $\dot{\theta}$ -pitch-up experiment of Walker et al. (1985) is simulated using direct numerical simulation and an unsteady NS analysis. The preliminary results obtained so far provide the flow structure and the evidence that eruption of secondary counterclockwise vortex near the quarter chord point triggers the formation of the dynamic stall vortex. However, additional results are essential to obtain the budget of vorticity dynamics and to shed further insight into this mechanism underlying the evolution of dynamic stall vortex just stated and its relation to unsteady separation. Based on the existing results of a video presentation of the numerically simulated evolution, convection and shedding

of the dynamic stall vortex is created, but for quantitative information comprehensive data is needed. It should be added that, in the earlier results for flow past a static Joukowski airfoil at 53° , the authors have seen the formation of a secondary counterclockwise vortex before the leading edge shear layer forms a large clockwise spinning vortex.

REFERENCES

1. Blodgett, G.A. Osswald, K.N. Ghia, U. Ghia, (1990), "Bubbles - An Unsteady Numerical Particle Trace Technique," to be presented at Sixteenth Annual AIAA Mini-Symposium on Aerospace Science and Technology, March, Dayton, Ohio.
2. Carr, L.W., (1988), "Progress in Analysis and Prediction of Dynamic Stall," Journal of Aircraft, Vol. 25, No. 1, pp. 6-17.
3. Ekaterinaris, J.A., (1989), "Compressible Studies on Dynamic Stall," AIAA Paper 89-0024, 27th Aerospace Sciences Meeting, Reno, Nevada, January 9-12.
4. Ghia, K.N., Osswald, G.A., and Ghia, U., (1985), "Analysis of Two-Dimensional Incompressible Flow Past Airfoils Using Unsteady Navier-Stokes Equations," Chapter in Numerical and Physical Aspects of Aerodynamic Flows, Vol. III, Editor: T. Cebeci, Springer-Verlag, New York, January.
5. Helin, H.E., (1989), "The Relevance of Unsteady Aerodynamics for Highly Maneuverable and Agile Aircraft," Proceedings of fourth symposium on Numerical and Physical Aspects of Aerodynamic Flows, Long Beach, California, January.
6. Osswald, G.A., Ghia, K.N. and Ghia, U., (1985), "An Implicit Time-Marching Method for Studying Unsteady Flow with Massive Separation," AIAA CP 854, pp. 25-37.
7. Osswald, G.A., Ghia, K.N., and Ghia, U., (1989), "Analysis of Potential and Viscous Flows Past Arbitrary Two-Dimensional Bodies with Sharp Trailing Edges," AIAA CP 895, pp. 668-677.
8. Visbal, M.R., and Shang, J.S., (1988), "Numerical Investigation of the Flow Structure Around a Rapidly Pitching Airfoil," "Proceedings of AFOSR/FJSRL/DFAM/UC Workshop II on Unsteady Separated Flows", FJSRL-TR-88-0004, pp. 91-108, September.
9. Walker, J.M., Helin, H.E., and Strickland, J.H., (1985), "An Experimental Investigation of an Airfoil Undergoing Large Amplitude Pitching Motions," AIAA Journal, Vol. 23, No. 8, pp. 1141-1142, August.

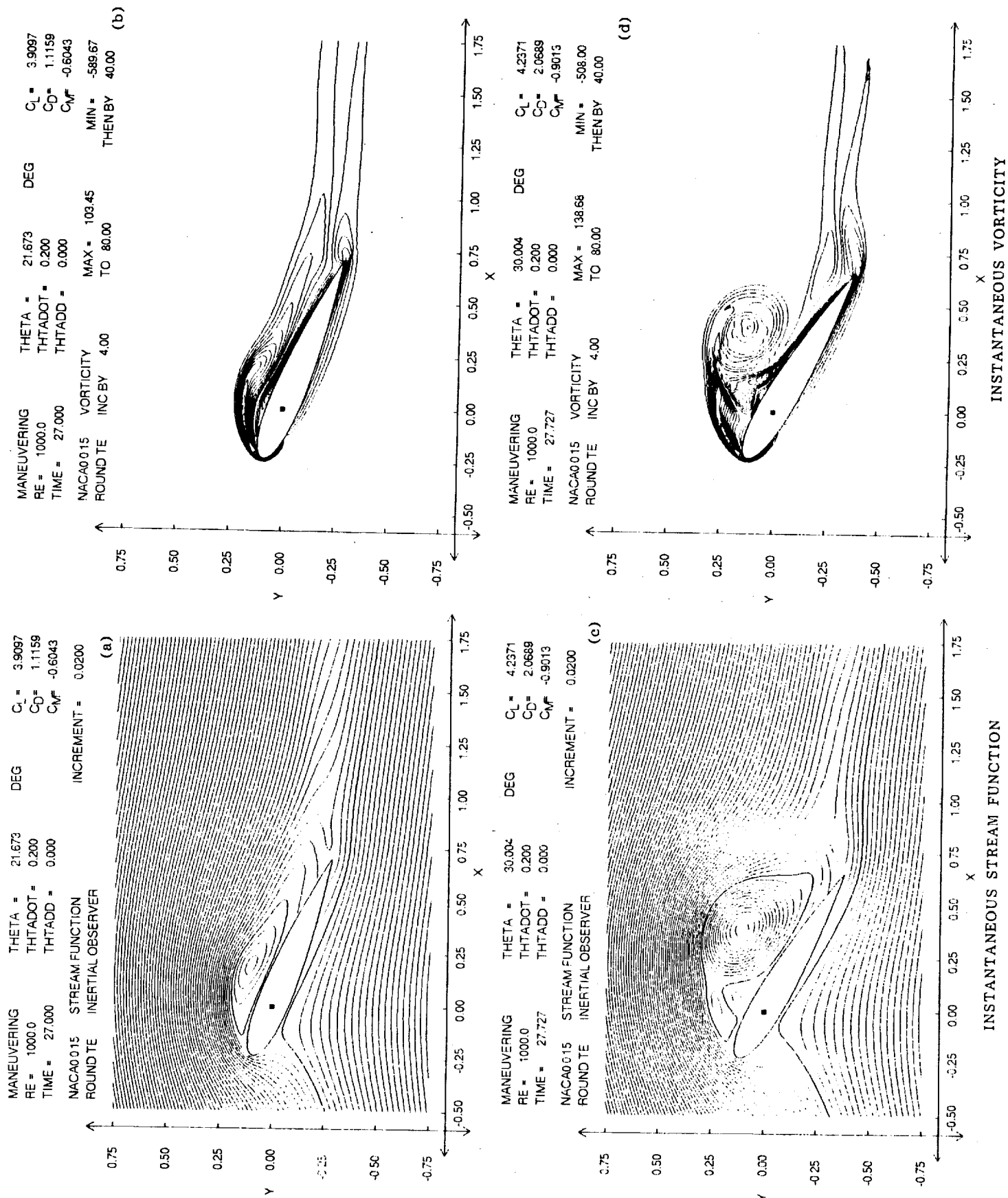


FIG. 1 CONTOURS OF INSTANTANEOUS STREAM FUNCTION AND VORTICITY DEPICTING DYNAMIC STALL.
Re = 1.000, (a-b) $\alpha = 21.673^\circ$, (c-d) $\alpha = 30.004^\circ$.

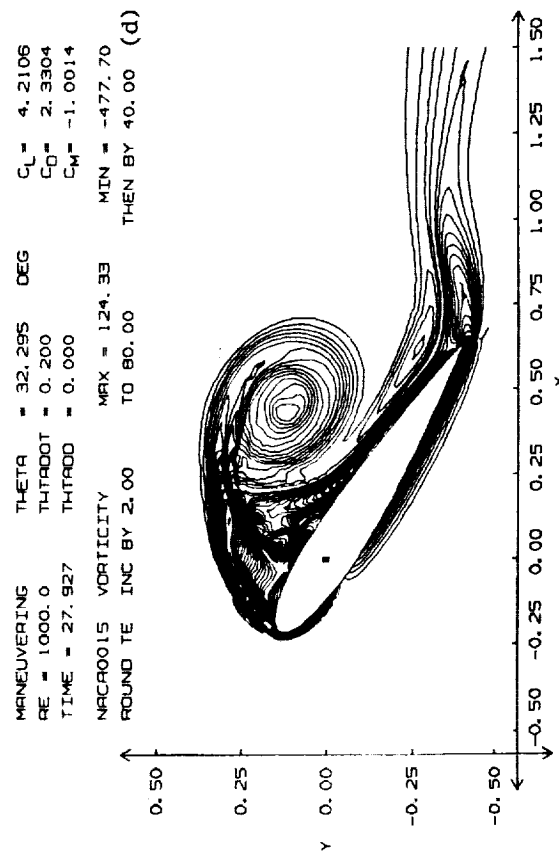
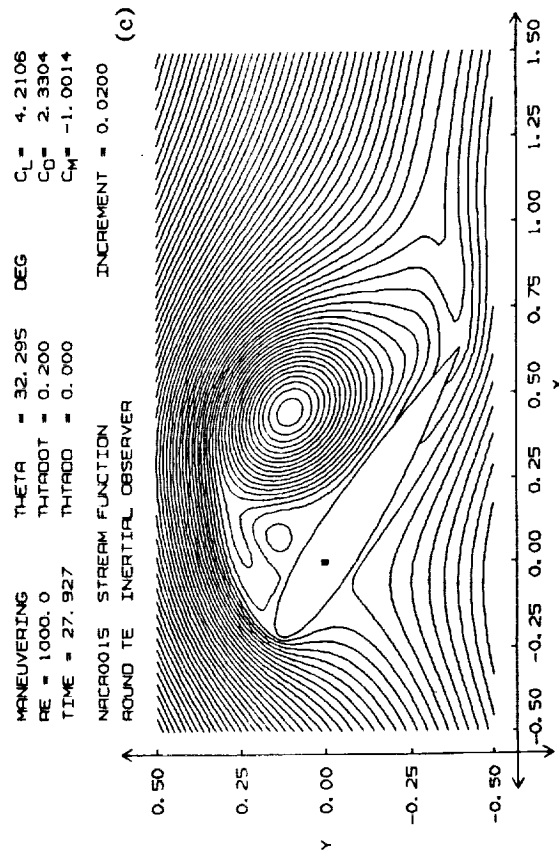
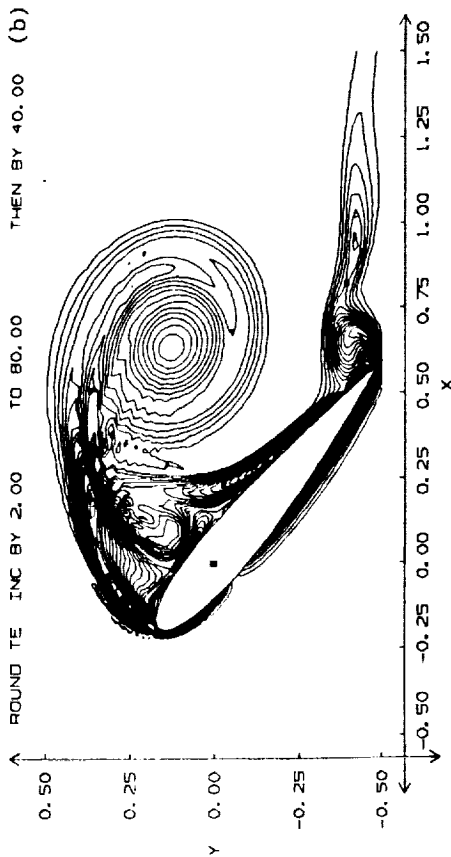
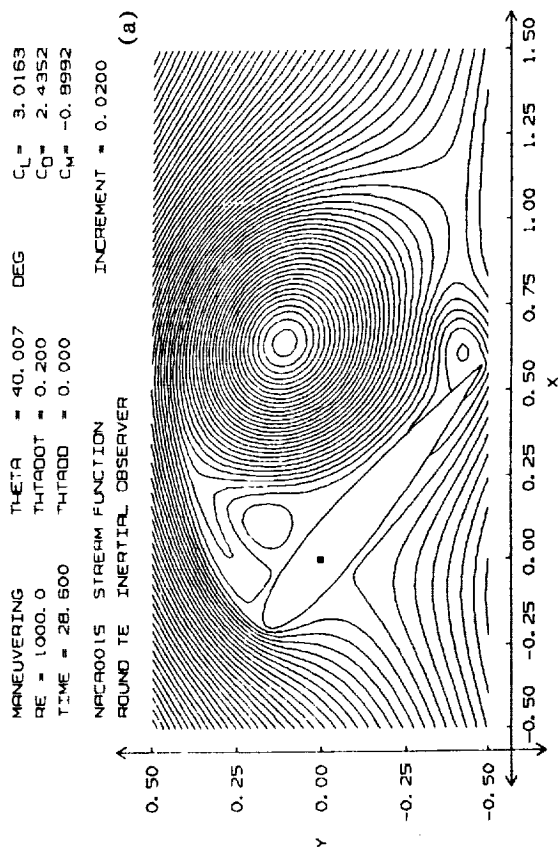


FIG. 1 CONT. CONTOURS OF INSTANTANEOUS STREAM FUNCTION AND VORTICITY DEPICTING DYNAMIC STALL.
 Re = 1,000, (a-b) $\alpha = 40.007^\circ$, (c-d) $\alpha = 32.295^\circ$.

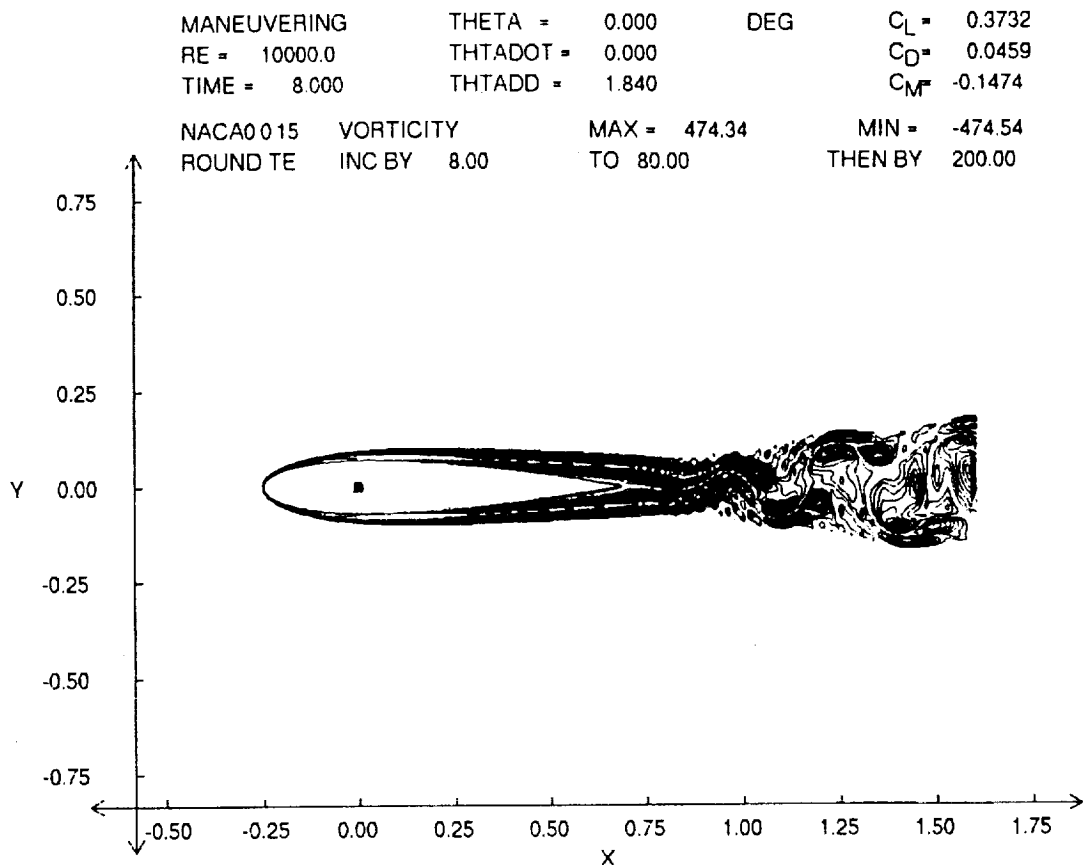


FIG. 2 VORTICITY CONTOURS FOR FLOW PAST A NACA0015 AIRFOIL,
 $Re = 10,000$, $\alpha = 0^\circ$, $t = 8.00$.

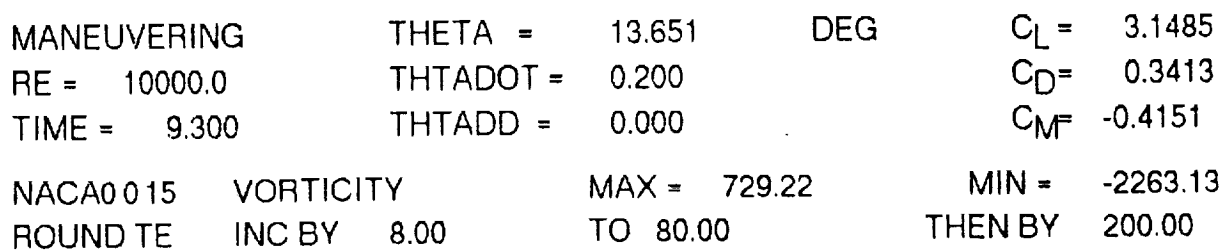
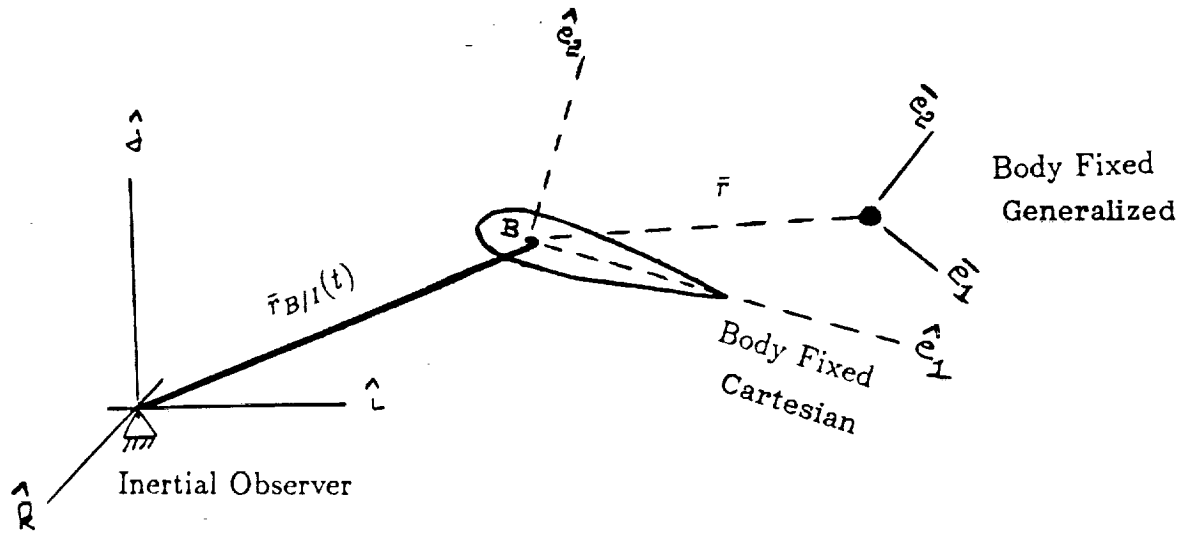


FIG. 2 CONT. ENLARGED VIEW OF LEADING EDGE DEPICTING EVOLUTION OF
 DYNAMIC STALL, $Re = 10,000$, $\alpha = 13.651^\circ$.

INERTIAL VS BODY FIXED OBSERVER



	Inertial Observer	Body Fixed Observer (Apparent)
Position of Fluid Particle:	\bar{r}_I	\bar{r}
Velocity of Fluid Particle:	\bar{V}_I	\bar{V}
Acceleration:	\bar{a}_I	\bar{a}
Vorticity:	$\bar{\omega}_I = \nabla \times \bar{V}_I$	$\bar{\omega} = \nabla \times \bar{V}$

KINEMATICS

$$\bar{r}_I = \bar{r}_{B/I}(t) + \bar{r}$$

$$\bar{V}_I = \bar{V}_{B/I}(t) + \bar{V} + \bar{\Omega}_B(t) \times \bar{r}$$

$$\bar{a}_I = \bar{a}_{B/I}(t) + \bar{a} + 2\bar{\Omega}_B(t) \times \bar{V} + \bar{\alpha}_B(t) \times \bar{r} + \bar{\Omega}_B(t) \times \bar{\Omega}_B(t) \times \bar{r}$$

$$\begin{aligned} \bar{\omega}_I &= \nabla \times \{\bar{V}_{B/I}(t) + \bar{V} + \bar{\Omega}_B(t) \times \bar{r}\} \\ &= 0 + \nabla \times \bar{V} + 2\bar{\Omega}_B(t) \\ &= \bar{\omega} + 2\bar{\Omega}_B(t) \end{aligned}$$

Arbitrary Maneuver Defined by:

$$\bar{r}_{B/I}(t)$$

$$\bar{V}_{B/I}(t) = \frac{d\bar{r}_{B/I}}{dt}$$

$$\bar{a}_{B/I}(t) = \frac{d^2\bar{r}_{B/I}}{dt^2}$$

$$\bar{\Omega}_B(t)$$

$$\bar{\alpha}_B(t) = \frac{d\bar{\Omega}_B}{dt}$$

UNSTEADY INCOMPRESSIBLE NAVIER-STOKES EQUATIONS

INERTIAL OBSERVER

PRIMITIVE VARIABLES

Continuity

$$\nabla \cdot \bar{V}_I = 0$$

Linear Momentum (Bernoulli's Form)

$$\frac{\partial \bar{V}_I}{\partial t} + (\nabla \times \bar{V}_I) \times \bar{V}_I + \frac{1}{Re} (\nabla \times \nabla \times \bar{V}_I) = -\nabla \left(p + \frac{|\bar{V}_I|^2}{2} \right)$$

VELOCITY-VORTICITY

Continuity

$$\nabla \cdot \bar{V}_I = 0$$

Kinematic Definition of Vorticity

$$\nabla \times \bar{V}_I = \bar{\omega}_I$$

Vorticity Transport

$$\frac{\partial \bar{\omega}_I}{\partial t} + \nabla \times (\bar{\omega}_I \times \bar{V}_I) + \frac{1}{Re} (\nabla \times \nabla \times \bar{\omega}_I) = 0$$

UNSTEADY INCOMPRESSIBLE NAVIER-STOKES EQUATIONS

BODY FIXED (APPARENT) OBSERVER

PRIMITIVE VARIABLES

Continuity

$$\nabla \cdot \bar{V} = 0$$

Linear Momentum (Bernoulli's Form)

$$\underbrace{\frac{\partial \bar{V}}{\partial t} + \bar{\alpha}_B(t) \times \bar{r}} + \underbrace{(\nabla \times \bar{V}) \times \bar{V} + 2\bar{\Omega}_B(t) \times \bar{V} + \frac{1}{Re} (\nabla \times \nabla \times \bar{V})}_{-\nabla \left(p + \frac{|\bar{V}|^2}{2} + \bar{a}_{B/I}(t) \cdot \bar{r} - \frac{|\bar{\Omega}_B(t) \times \bar{r}|^2}{2} \right)} =$$

VELOCITY-VORTICITY

Continuity

$$\nabla \cdot \bar{V}_I = 0$$

Kinematic Definition of Vorticity

$$\nabla \times \bar{V}_I = \bar{\omega}_I$$

Vorticity Transport

$$\frac{\partial \bar{\omega}_I}{\partial t} + \nabla \times (\bar{\omega}_I \times \bar{V}) + \frac{1}{Re} (\nabla \times \nabla \times \bar{\omega}_I) = 0$$

Kinematic Relationship Between Apparent and Inertial Velocity

$$\bar{V} = \bar{V}_I - \bar{V}_{B/I}(t) - \bar{\Omega}_B(t) \times \bar{r}$$

- Solve For Inertial Velocity and Inertial Vorticity Directly in Body Fixed Frame
- Form of Governing Eqs. Unaltered

Inertial Velocity Boundary Conditions Remain Unaltered

Only Differences Are

- Inertial Vorticity Advects with Apparent Velocity
- Additional Vorticity is Created at Body Surface Due to Acceleration of Body

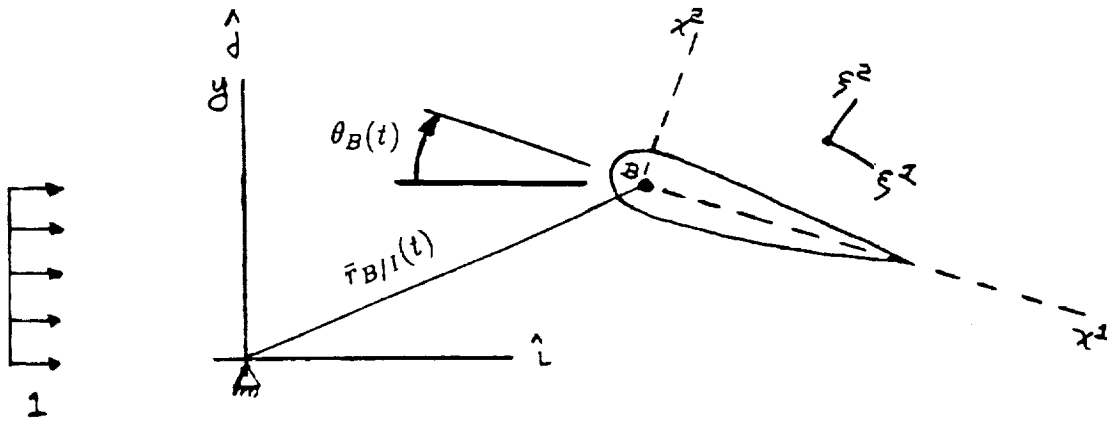
For Two-Dimensional Flow, use

DISTURBANCE STREAM FUNCTION-VORTICITY FORMULATION IN GENERALIZED BODY FIXED COORDINATES

Definition of Disturbance Stream Function (Deviation from Uniform Flow)

$$\psi_{INERTIAL} = [y + \Psi_o] + \psi_I^{DIS}(\xi^1, \xi^2, t)$$

Where Ψ_o is at yet an Unknown Integration Constant Representing a Displacement of the ZERO STREAMLINE at INFINITY



Arbitrarily Maneuvering

$$\psi_{INERTIAL} = [x^2 \cos \theta(t) - x^1 \sin \theta(t) + \Psi_o] + \psi_I^{DIS}(\xi^1, \xi^2, t)$$

ELLIPTIC STREAM FUNCTION PROBLEM

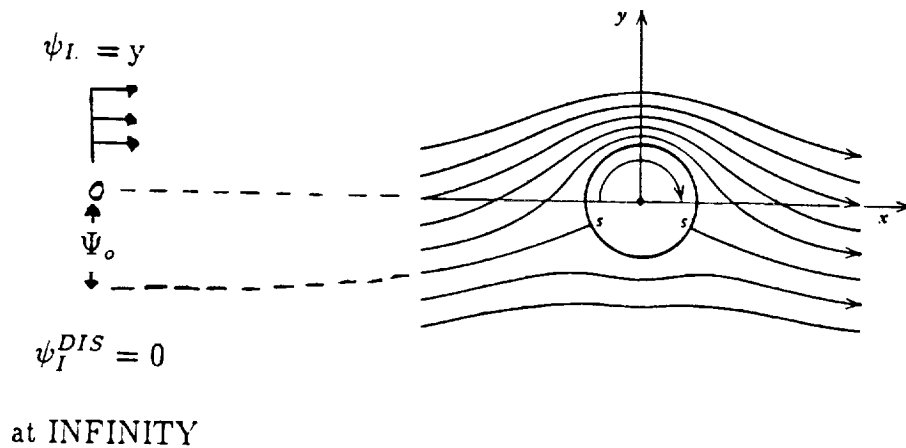
$$\frac{\partial}{\partial \xi^1} \left(\frac{g_{22}}{\sqrt{g}} \frac{\partial \psi_I^{DIS}}{\partial \xi^1} \right) + \frac{\partial}{\partial \xi^2} \left(\frac{g_{11}}{\sqrt{g}} \frac{\partial \psi_I^{DIS}}{\partial \xi^2} \right) = -\sqrt{g} \omega_I^3$$

Subject to the Boundary Conditions

$$\psi_I^{DIS} = 0 \text{ at INFINITY}$$

$$\psi_I^{DIS} = \{x^2[V_{B/I}^1(t) - \cos \theta(t)] - x^1[V_{B/I}^2(t) - \sin \theta(t)] - \frac{\Omega_B(t)}{2}[(x^1)^2 + (x^2)^2]\}$$

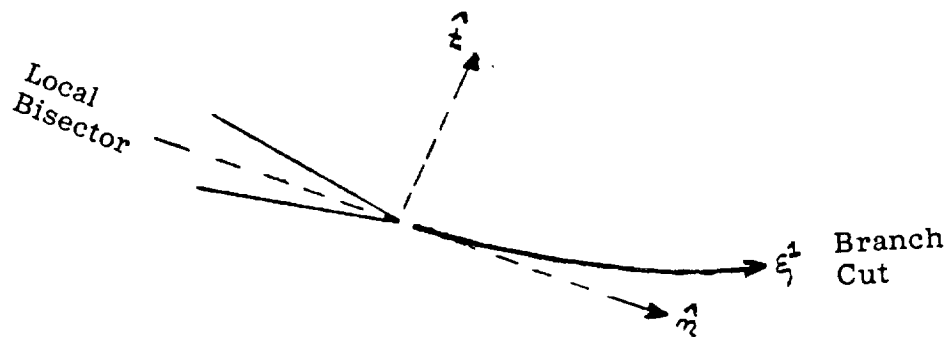
Along Body Surface



STRICTLY AN INVISCID EFFECT (ALL VISCOUS
DISTURBANCES DISSIPATE WELL BEFORE INFINITY)

DIRECTLY REPRESENTS UNDERLYING INVISCID
CIRCULATION SET BY AN INVISCID KUTTA CONDITION AT
TRAILING EDGE

KUTTA CONDITION FOR Ψ_o (WEDGE TRAILING EDGE)



$$\lim_{\substack{\vec{TE} \\ BRANCH CUT}} \left\{ \frac{1}{\sqrt{g_{11}}} \frac{\partial \psi_{INVISCID}^{DIS}}{\partial \xi^1} \right\} =$$

$$\left[\{ \cos \theta(t) - V_{B/I}^1(t) + x^2 \Omega_B(t) \} \hat{e}_1 + \{ \sin \theta(t) - V_{B/I}^2(t) - x^1 \Omega_B(t) \} \hat{e}_2 \right] \cdot \hat{t}$$

VORTICITY TRANSPORT

$$\begin{aligned} \sqrt{g} \frac{\partial \omega_I^3}{\partial t} + \frac{\partial}{\partial \xi^1} (\omega_I^3 [\sqrt{g} V^1]) + \frac{\partial}{\partial \xi^2} (\omega_I^3 [\sqrt{g} V^2]) = \\ \frac{1}{Re} \left\{ \frac{\partial}{\partial \xi^1} \left(\frac{g_{22}}{\sqrt{g}} \frac{\partial \omega_I^3}{\partial \xi^1} \right) + \frac{\partial}{\partial \xi^2} \left(\frac{g_{11}}{\sqrt{g}} \frac{\partial \omega_I^3}{\partial \xi^2} \right) \right\} \end{aligned}$$

where

$$\begin{aligned} \sqrt{g} V^1 &= \frac{[\{\cos \theta(t) - V_{B/I}^1(t) + x^2 \Omega_B(t)\} \hat{e}_1 + \{\sin \theta(t) - V_{B/I}^2(t) - x^1 \Omega_B(t)\} \hat{e}_2] \cdot \bar{e}_1}{g_{11}/\sqrt{g}} + \frac{\partial \psi_I^{DIS}}{\partial \xi^2} \\ \sqrt{g} V^2 &= \frac{[\{\cos \theta(t) - V_{B/I}^1(t) + x^2 \Omega_B(t)\} \hat{e}_1 + \{\sin \theta(t) - V_{B/I}^2(t) - x^1 \Omega_B(t)\} \hat{e}_2] \cdot \bar{e}_2}{g_{22}/\sqrt{g}} + \frac{\partial \psi_I^{DIS}}{\partial \xi^1} \end{aligned}$$

Subject to the Boundary Condition

$$\omega_I^3 = 0 \quad \text{at Infinity}$$

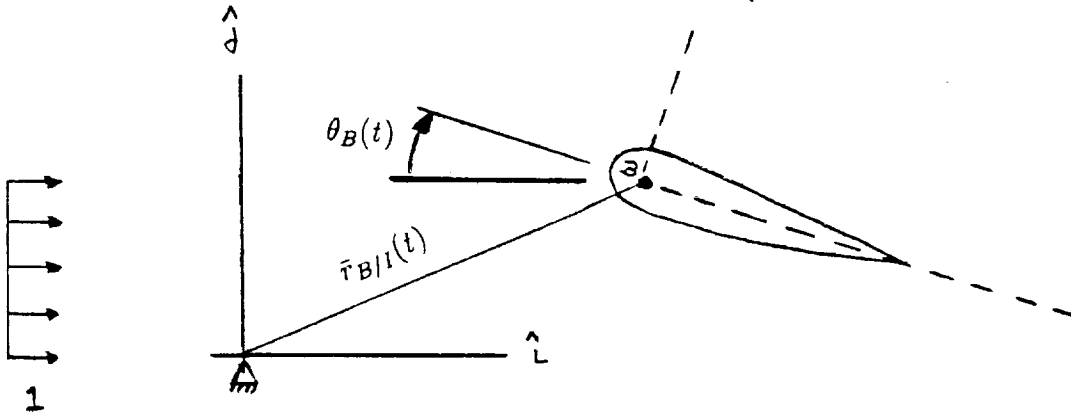
and Along the Body

$$-\sqrt{g} \omega_I^3 = \frac{\partial}{\partial \xi^1} \left(\frac{g_{22}}{\sqrt{g}} \frac{\partial \psi_I^{DIS}}{\partial \xi^1} \right) + \frac{\partial}{\partial \xi^2} \left(\frac{g_{11}}{\sqrt{g}} \frac{\partial \psi_I^{DIS}}{\partial \xi^2} \right)$$

Subject to the Constraint

$$\frac{g_{11}}{\sqrt{g}} \frac{\partial \psi_I^{DIS}}{\partial \xi^2} = [\{\cos \theta(t) - V_{B/I}^1(t) + x^2 \Omega_B(t)\} \hat{e}_1 + \{\sin \theta(t) - V_{B/I}^2(t) - x^1 \Omega_B(t)\} \hat{e}_2] \cdot \bar{e}_2$$

THE PITCH UP MANEUVER OF VISBAL AND SHANG



$$\bar{r}_{B/I}(t) = 0$$

$$\bar{V}_{B/I}(t) = 0$$

$$\bar{a}_{B/I}(t) = 0$$

$$\theta_B(t) = \Omega_o \left[t - \left(\frac{t_o}{4.6} \right) (1 - \exp - \left(\frac{4.6}{t_o} \right) t) \right]$$

$$\Omega_B(t) = -\Omega_o \left(1 - \exp - \left(\frac{4.6}{t_o} \right) t \right)$$

$$\alpha_B(t) = - \left(\frac{4.6}{t_o} \right) \Omega_o \exp - \left(\frac{4.6}{t_o} \right) t$$

Where

Ω_o - Nondimensional Pitch Rate; 0.2

t_o - Nondimensional Acceleration Time; 0.5

x_o - Pivot Axis Location Measured from Airfoil LE; 0.25

SUMMARY

- Developed Navier-Stokes Analysis for forced unsteady separated flow using stream function and vorticity; the latter is the variable of the greatest physical significance.
- Based on the present analysis. Here is our response to some of the questions posed.

◦ What is the process whereby fluid particles in the vicinity of the wall are ejected from that region and coalesce into an outer-layer vortex structure?	→	Formation of counterclockwise vortex in boundary layer leads to formation of dynamic stall vortex.
◦ How is this mechanism modified by transitional effects? Compressibility? Turbulence? Three-dimensionality? Surface Curvature? Suction or blowing?	→	Future work with this analysis will help to answer part of this question.
◦ Is the unsteady separation phenomenon associated with dynamic stall <u>unique</u> to rapidly pitching wings, or <u>can it be</u> studied on fixed surfaces as well?	→	No, the phenomenon is not unique. Our results for the stationary Joukowski airfoil at very high angle of attack show a similar flow structure.
◦ Can we detect incipient breakdown of the attached shear layer in time to influence or delay detachment?	→	It appears that it is possible to delay detachment.
◦ Is it realistic to hope to suppress unsteady separation, or should we be spending our effort in controlling the flow after separation has occurred?	→	?
◦ Dynamic stall has been observed on airfoils experiencing leading-edge stall, as well as trailing-edge stall. Is the unsteady separation mechanism different in these two cases?	→	We would like to conduct these experiments to accurately respond to this question.
◦ What will we need to know about the unsteady flow development in order to actually implement control technologies for suppression of unsteady separation on rapidly pitching wings?	→	—

